Electronic Supplementary Material (ESI) for Dalton Transactions.

Electronic Supporting Information for:

Dynamic porous coordination polymers built-up from flexible 4,4′-dithiodibenzoate and rigid N-based ligands

Najmeh Jarrah,[a,b] Javier Troyano,[*a] Arnau Carne,[a] Inhar Imaz,[a] Shahram Tangestaninejad,[b] Majid Moghadam[*b] and Daniel Maspoch[*a,c]

[a] Catalan Institute of Nanoscience and Nanotechnology (ICN2), Campus UAB, Bellaterra, 08193 Barcelona, Spain

[b] Department of Chemistry, University of Isfahan, Isfahan 81746-73441, Iran

[c] ICREA, Pg. Lluís Companys 23, 08010 Barcelona, Spain

Table S1. Data collection and structure refinement for **1**

Identification code	**1**
Empirical formula	$C_{18.5}H_{18.5}CuN_{1.5}O_{5.5}S_2$
Formula weight	477.51
Temperature/K	100
Crystal system	triclinic
Space group	*P*-1
a/Å	9.960(5)
b/Å	10.210(5)
c/Å	12.060(5)
α/°	102.901(5)
β/°	100.793(5)
γ/°	113.618(5)
Volume/Å^3	1041.4(8)
Z	2
ρ_{calc}g/cm^3	1.523
μ/mm^{-1}	1.431
F(000)	490.0
Crystal size/mm^3	0.22 × 0.15 × 0.1
Radiation	synchrotron (λ = 0.82653)
2Θ range for data collection/°	5.368 to 67.692
Index ranges	$-13 \leq h \leq 12$, $-12 \leq k \leq 12$, $-16 \leq l \leq 16$
Reflections collected	3976
Independent reflections	3976 [R_{int} = ?, R_{sigma} = 0.0641]
Data/restraints/parameters	3976/1/276
Goodness-of-fit on F^2	1.055
Final R indexes [I>=2σ (I)]	R_1 = 0.0710, wR_2 = 0.2099
Final R indexes [all data]	R_1 = 0.0753, wR_2 = 0.2146
Largest diff. peak/hole / e Å^{-3}	1.68/-0.74

Table S2. Data collection and structure refinement for **2**

Identification code	**2**
Empirical formula	$C_{39}H_{28.33}Cu_2N_{2.33}O_{8.33}S_4$
Formula weight	918.29
Temperature/K	100
Crystal system	triclinic
Space group	*P*-1
a/Å	10.390(6)
b/Å	21.680(6)
c/Å	21.910(6)
α/°	115.86(5)
β/°	103.91(5)
γ/°	93.65(5)
Volume/Å^3	4230(3)
Z	3
ρ_{calc}g/cm^3	1.081
μ/mm^{-1}	1.422
F(000)	1402.0
Crystal size/mm^3	0.24 × 0.23 × 0.21
Radiation	synchrotron (λ = 0.82643)
2Θ range for data collection/°	2.474 to 67.626
Index ranges	$-13 \le h \le 13$, $-25 \le k \le 25$, $-28 \le l \le 29$
Reflections collected	38580
Independent reflections	16297 [R_{int} = 0.1310, R_{sigma} = 0.1583]
Data/restraints/parameters	16297/46/751
Goodness-of-fit on F^2	0.940
Final R indexes [I>=2σ (I)]	R_1 = 0.0973, wR_2 = 0.2659
Final R indexes [all data]	R_1 = 0.1629, wR_2 = 0.3106
Largest diff. peak/hole / e Å^{-3}	0.73/-1.10

Table S3. Data collection and structure refinement for **3**

Identification code	**3**
Empirical formula	$C_{18}H_{12}NO_4S_2Cu$
Formula weight	433.95
Temperature/K	293(2)
Crystal system	monoclinic
Space group	*C*2/*c*
a/Å	24.3747(7)
b/Å	13.9313(3)
c/Å	18.9465(7)
α/°	90
β/°	111.435(4)
γ/°	90
Volume/Å^3	5988.7(3)
Z	13
ρ_{calc}g/cm^3	1.564
μ/mm^{-1}	1.434
F(000)	2860.0
Crystal size/mm^3	0.02 × 0.02 × 0.15
Radiation	MoKα (λ = 0.71073)
2Θ range for data collection/°	3.752 to 62.85
Index ranges	$-24 \le h \le 35$, $-20 \le k \le 19$, $-27 \le l \le 26$
Reflections collected	35765
Independent reflections	9032 [R_{int} = 0.0326, R_{sigma} = 0.0319]
Data/restraints/parameters	9032/0/294
Goodness-of-fit on F^2	1.069
Final R indexes [I>=2σ (I)]	R_1 = 0.0619, wR_2 = 0.1775
Final R indexes [all data]	R_1 = 0.0747, wR_2 = 0.1854
Largest diff. peak/hole / e Å^{-3}	1.64/-0.85

Table S4. Data collection and structure refinement for **4**

Identification code	**4**
Empirical formula	$C_{34}H_{24}Cu_2N_6O_{10}S_2$
Formula weight	867.79
Temperature/K	180
Crystal system	monoclinic
Space group	$P2_1/m$
a/Å	8.9361(4)
b/Å	24.6960(15)
c/Å	10.4597(4)
α/°	90
β/°	110.946(4)
γ/°	90
Volume/Å^3	2155.77(19)
Z	2
ρ_{calc}g/cm^3	1.337
μ/mm^{-1}	1.716
F(000)	880.0
Crystal size/mm^3	0.1 × 0.1 × 0.01
Radiation	MoKα (λ = 0.71073)
2Θ range for data collection/°	4.17 to 50.054
Index ranges	$-10 \le h \le 9$, $-29 \le k \le 29$, $-10 \le l \le 12$
Reflections collected	3908
Independent reflections	3908 [R_{int} = ?, R_{sigma} = 0.0277]
Data/restraints/parameters	3908/136/281
Goodness-of-fit on F^2	1.068
Final R indexes [I>=2σ (I)]	R_1 = 0.0880, wR_2 = 0.2652
Final R indexes [all data]	R_1 = 0.1039, wR_2 = 0.2797
Largest diff. peak/hole / e Å^{-3}	0.90/-0.54

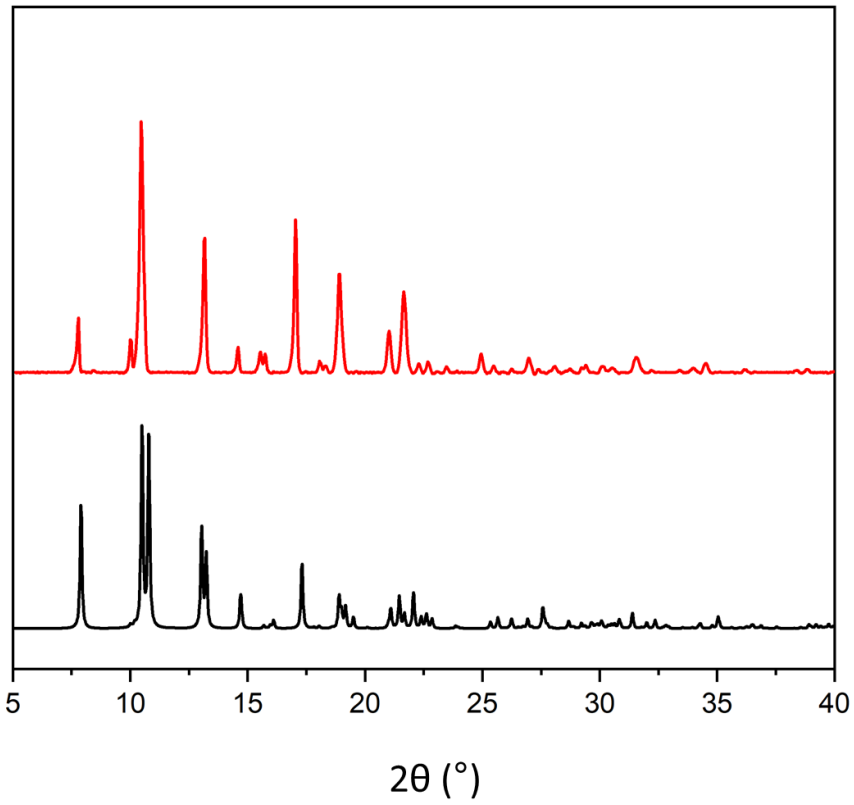

Figure S1. XRPD patterns of as-synthesized (red) and simulated (black) compound **1**.

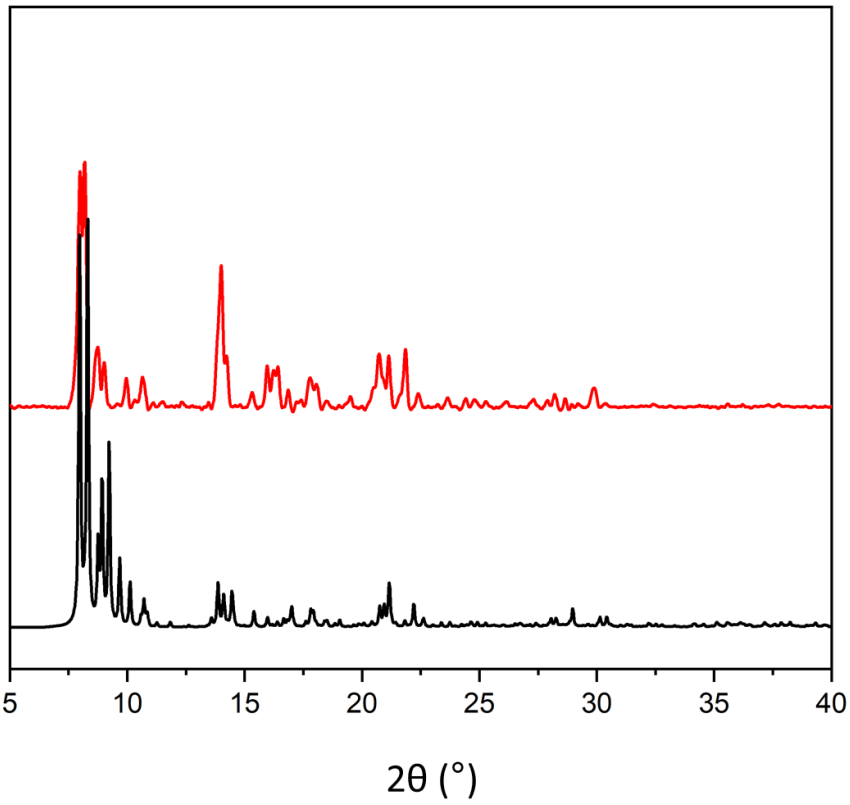

Figure S2. XRPD patterns of as-synthesized (red) and simulated (black) compound **2**.

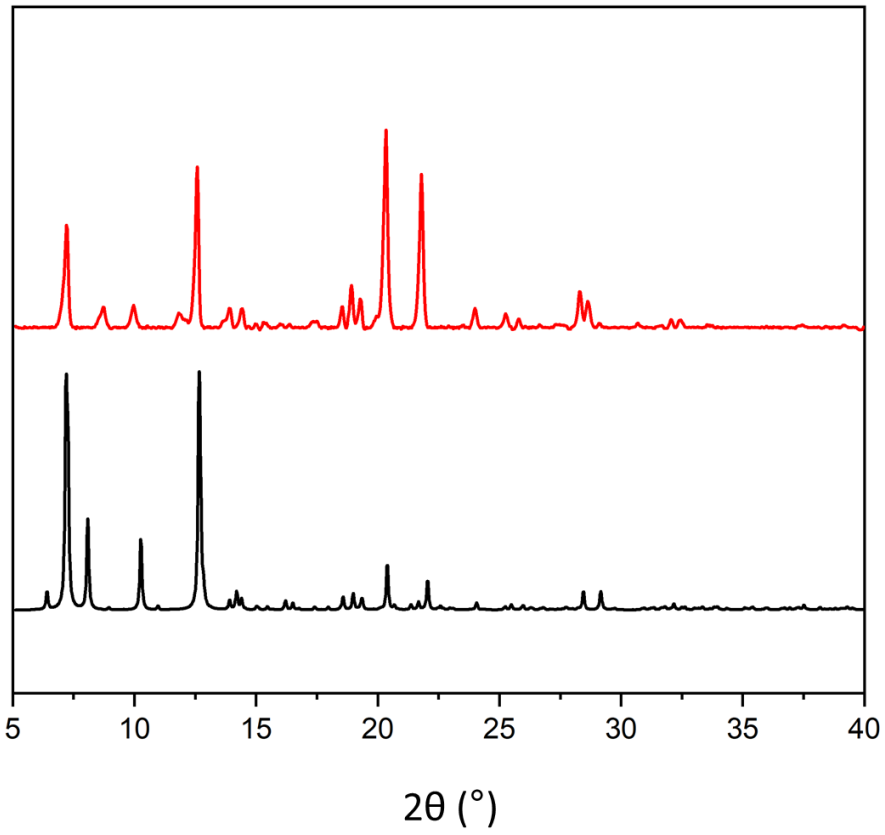

Figure S3. XRPD patterns of as-synthesized (red) and simulated (black) compound **3**.

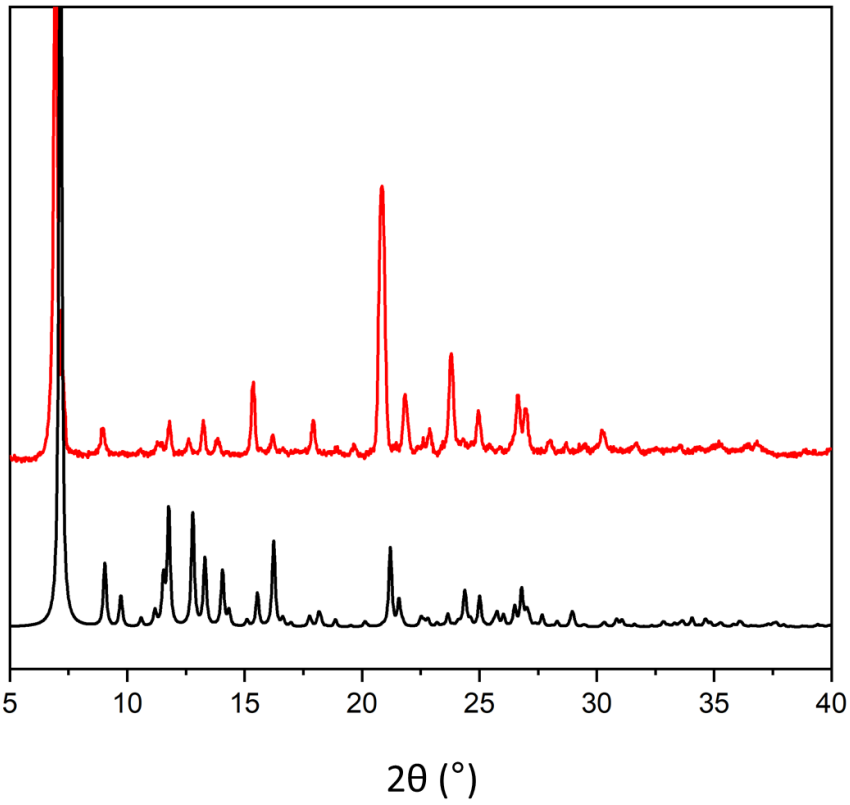

Figure S4. XRPD patterns of as-synthesized (red) and simulated (black) compound **4**.

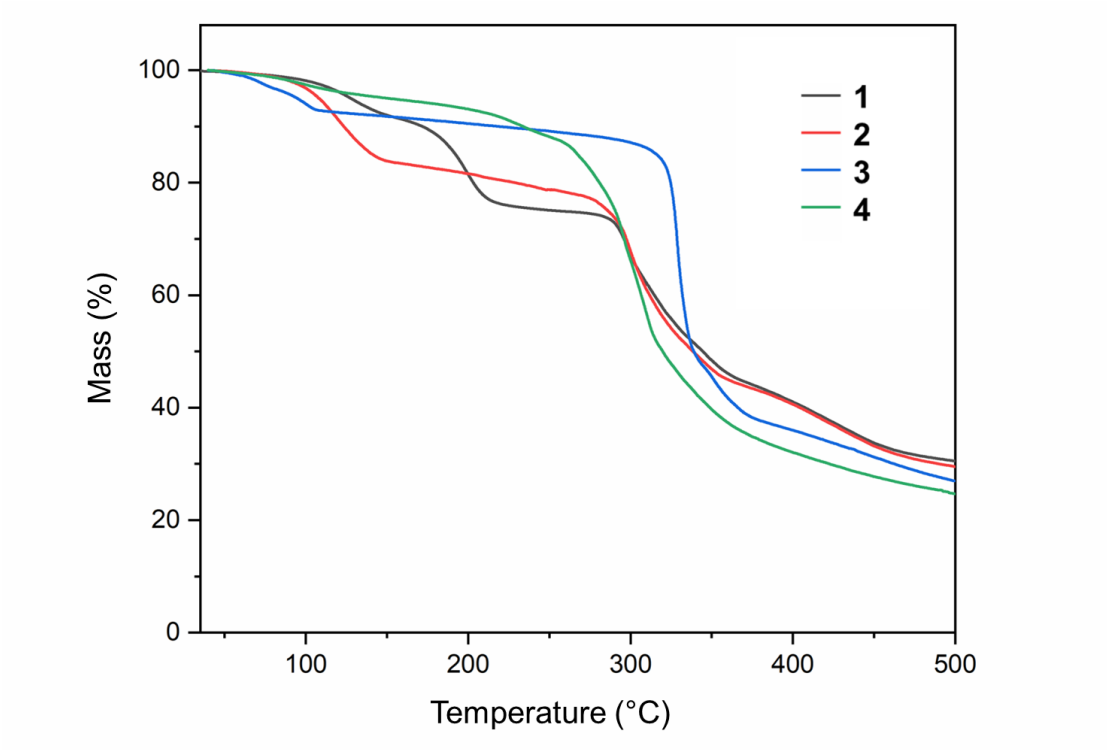

Figure S5. TGA curves of compounds **1-4** before solvent exchange in N_2 atmosphere with a heating rate of 5 °C min^{-1}.

Table S5. TGA data for compounds for compounds **1-4**

Compound	Proposed formula	Temperature range (°C)	% Mass loss (calc.)	Mass loss assignment
1	$[Cu(4,4'\text{-DTBA})(DMF)]_n \cdot 0.5DMF$	80-145	7.5 (7.7)	0.5 DMF
		160-220	16.3 (15.3)	1 DMF
		275	69.4	decomposition
2	$[Cu(4,4'\text{-DTBA})(py)]_n \cdot 0.33DMF$	70-275	77.9 (78.0)	py + 0.33 DMF
		275	70.5	decomposition
3	$[Cu_2(4,4'\text{-DTBA})_2(4,4'\text{-bpy})]_n \cdot 2DMF$	40-300	13.9 (14.1)	2 DMF
		300	73.1	decomposition
4	$[Cu_2(NO_3)_2(4,4'\text{-DTBA})(4,4'\text{-bpy})_2]_n$	250	72.5	decomposition

Table S6. Selected bond lengths and angles for compounds **1-4** and previously reported $[Cu_2(4,4'\text{-DTBA})(H_2O)_2]_n$ coordination polymers[1]

	Cu-Cu (Å)	Cu-O (Å)	Cu-N (Å)	S-S (Å)	C-S-S (°)	C-S-S-C torsion angle (°)	Dihedral angle (°)
1 $[Cu(4,4'\text{-DTBA})(DMF)]_n$	2.633(13)	1.951(3) 1.964(3) 1.965(3) 1.979(3) 2.146(4)		2.033(2)	105.50(18) 105.59(19)	69.8(3)	70.1(2)
2 $[Cu(4,4'\text{-DTBA})(py)]_n$	2.635(2) 2.645(2)	1.949(6) 1.954(6) 1.964(6) 1.968(6) 1.970(7) 1.978(5) 1.990(5) 1.999(6)	2.165(7) 2.173(7) 2.181(7)	2.015(5) 2.025(3) 2.036(4)	102.0(3) 103.0(4) 105.4(3) 105.5(4) 105.6(3) 105.8(3)	78.6(5) 83.6(6) 85.4(5)	75.0(4) 87.6(4) 100.0(3)
3 $[Cu_2(4,4'\text{-DTBA})_2(4,4'-bpy)]_n$	2.623(6)	1.947(2) 1.956(2) 1.964(2) 2.022(2)	2.126(3) 2.135(3)	2.022(11)	104.94(11) 105.04(11)	78.0(2)	82.81(12)
4 $[Cu_2(NO_3)_2(4,4'\text{-DTBA})(4,4'-bpy)_2]_n$		1.915(13) 2.030(2) 2.066(7) 2.102(16) 2.264(14)	2.017(6) 2.019(5)	1.374(13)	128.9(6) 129.6(6)	75.6(2)	84.6(6)
$[Cu_2(4,4'\text{-DTBA})(H_2O)_2]_n$ (1D)	2.647(2)	1.958(4) 1.972(6)		2.023(2)	105.92(2)	73.64(2)	73.02(3)
$[Cu_2(4,4'\text{-DTBA})(H_2O)_2]_n$ (2D)	2.609(1)	1.951(4) 1.958(4) 1.974(4) 1.983(4) 2.150(4)		2.020(2)	105.23(2) 105.98(2)	91.10(3)	78.40(3)

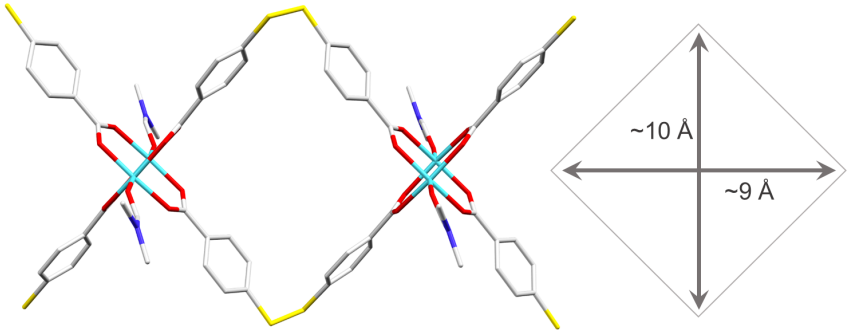

Figure S6. View of the square cavities formed in **1** showing the pore aperture dimensions.

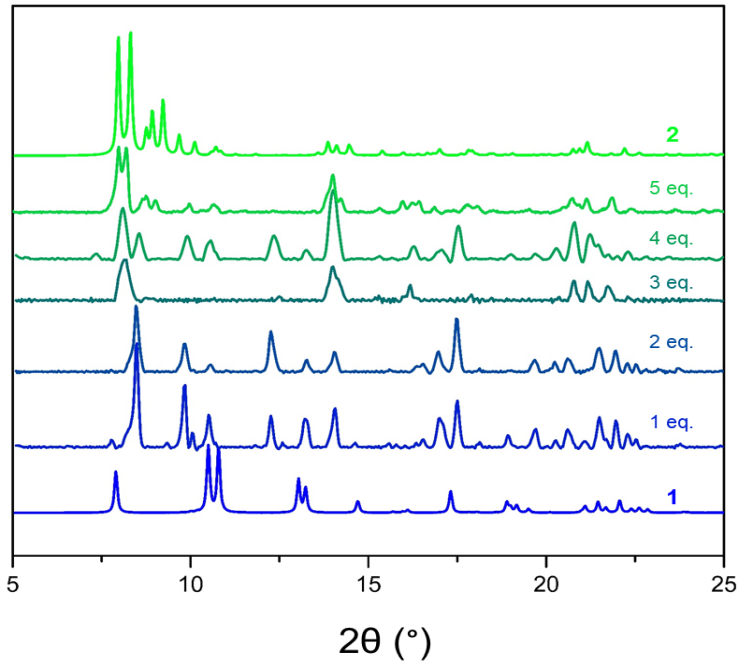

Figure S7. XRPD patterns of the solids obtained after reacting $Cu(NO_3)_2$ and 4,4´-DTBA in the presence of 1-5 equivalents of pyridine, compared with simulated patterns for **1** and **2**.

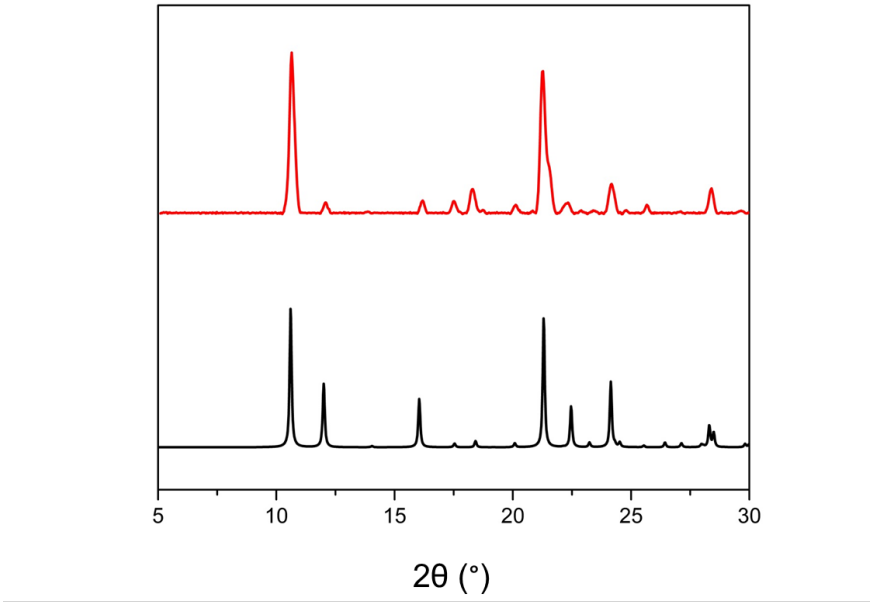

Figure S8. XRPD patterns of as-synthesized (red) and simulated (black) $[Cu(py)_4(NO_3)_2]\cdot 2py$ complex.[2]

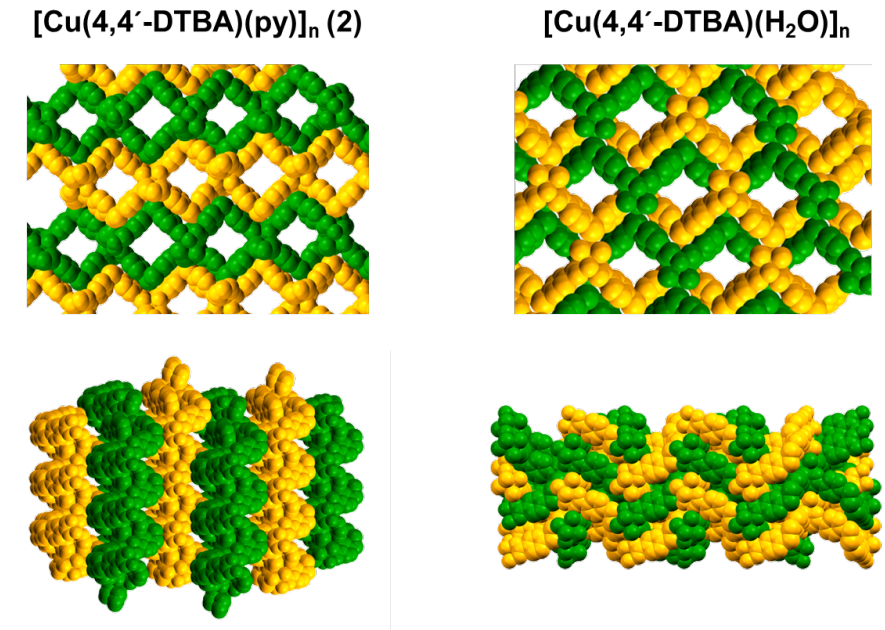

Figure S9. Space filling models of non-interpenetrated **2** (left) and previously reported 2-fold interpenetrated $[Cu_2(4,4´\text{-DTBA})(H_2O)_2]_n$[1] (right) showing the crystal packing of 2D layers in which the various colours differentiates the contiguous layers.

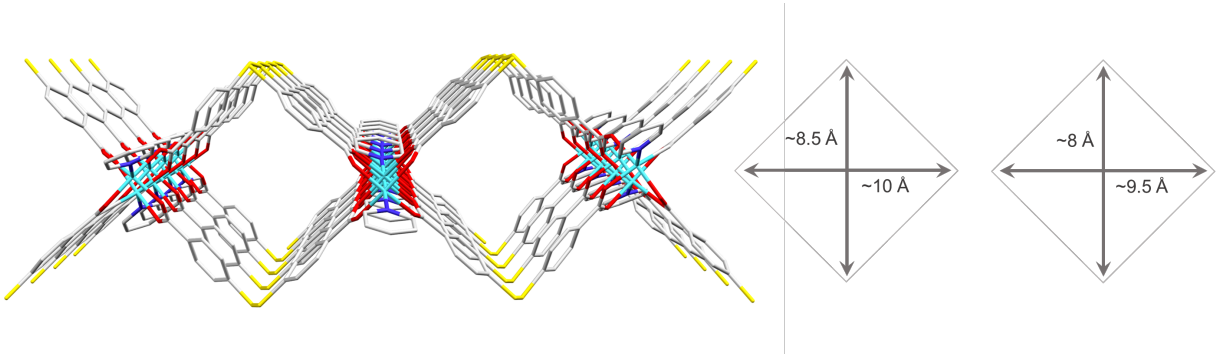

Figure S10. View of the square channels formed in **2** showing the pore aperture dimensions.

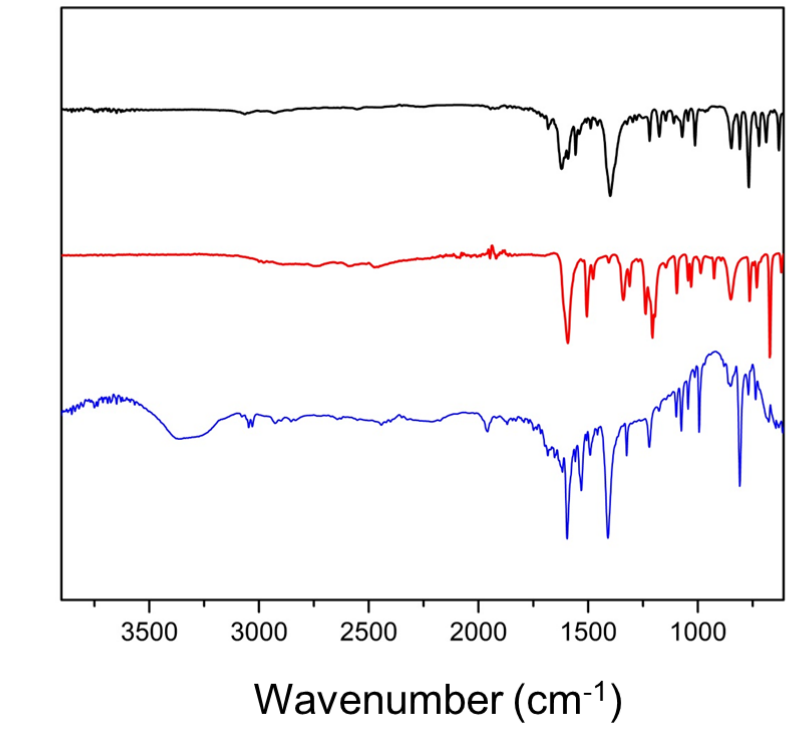

Figure S11. FT-IR spectra of **3´** (black), 4,4´-DTBA (red) and 4,4´-bpy (blue).

Table S7. CHNS Elemental analysis of **3´** and theoretical values for a $Cu_2(4,4´\text{-DTBA})_2(4,4´\text{-bpy})$ composition

	C (%)	H (%)	N (%)	S (%)
3´	50.77	2.64	3.08	14.19
$C_{19}H_{12}CuNO_4S_2$ (*calcd.*)	51.17	2.71	3.14	14.38

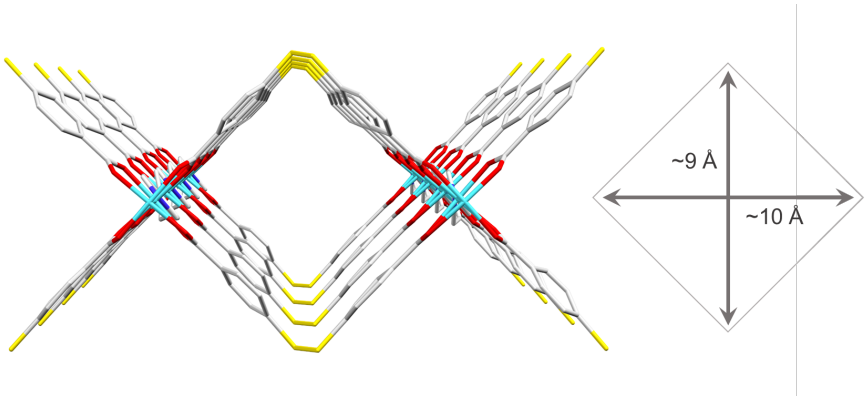

Figure S12. View of the square channels formed in **3** showing the pore aperture dimensions.

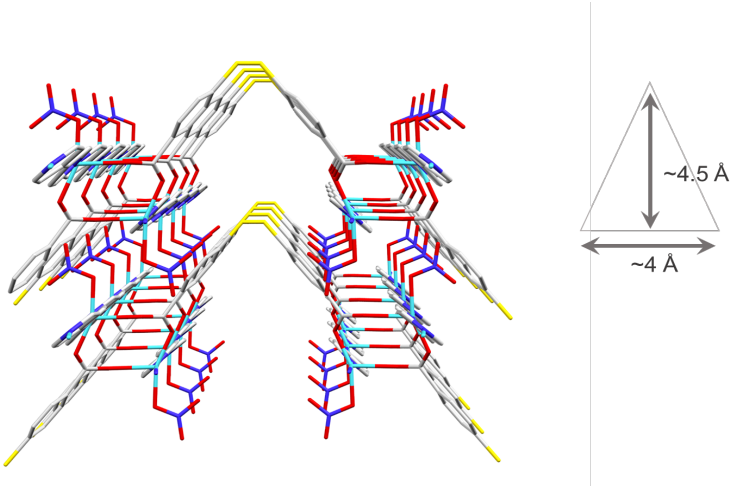

Figure S13. View of the triangular pore aperture of 2D porous channels in **4** showing the pore aperture dimensions.

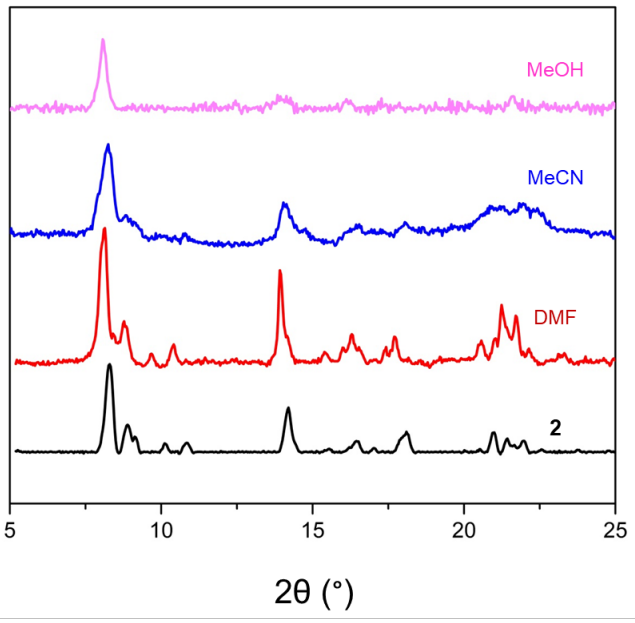

Figure S14. XRPD patterns of **2** after immersing in various solvents for 48 h at room temperature.

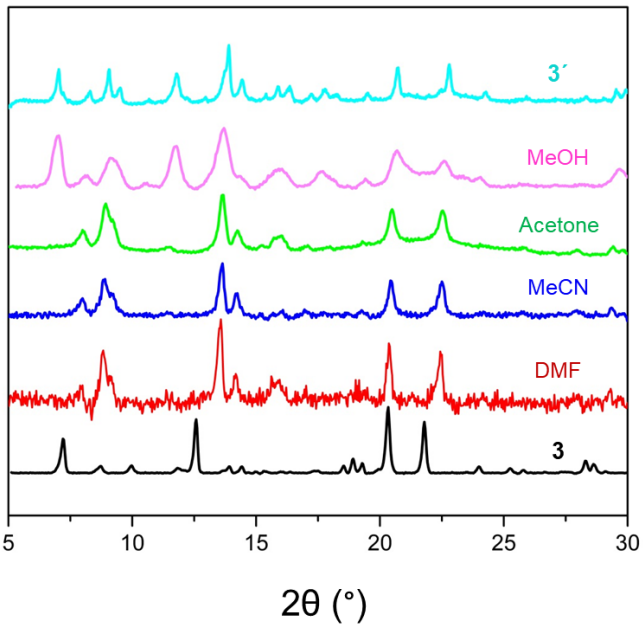

Figure S15. XRPD patterns of **3** after immersing in various solvents 48 h at room temperature.

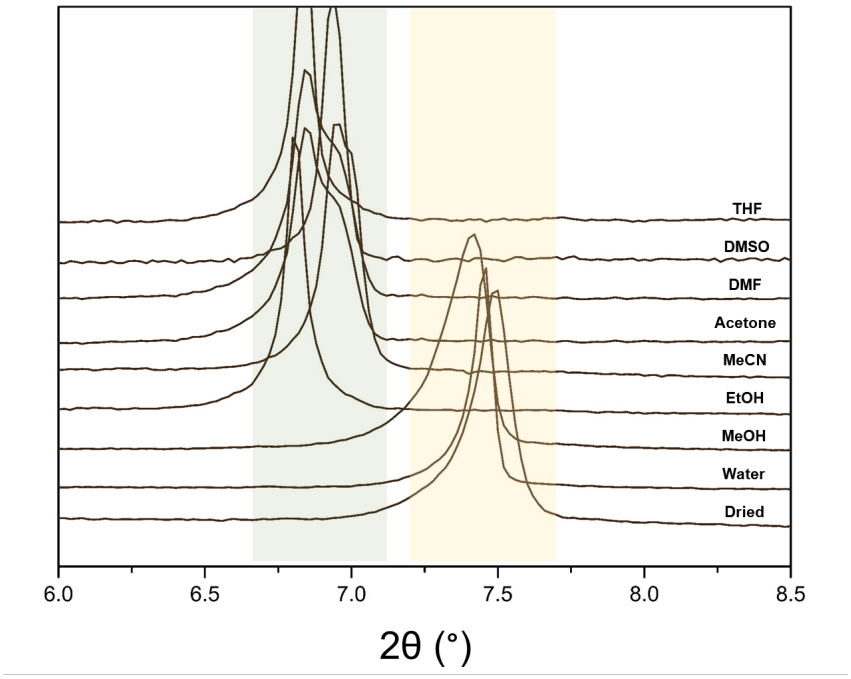

Figure S16. Zoom of the recorded XRPD patterns of **4′** before (dried) and after immersion in water and several organic solvents in the region 6°<2θ<8.5°.

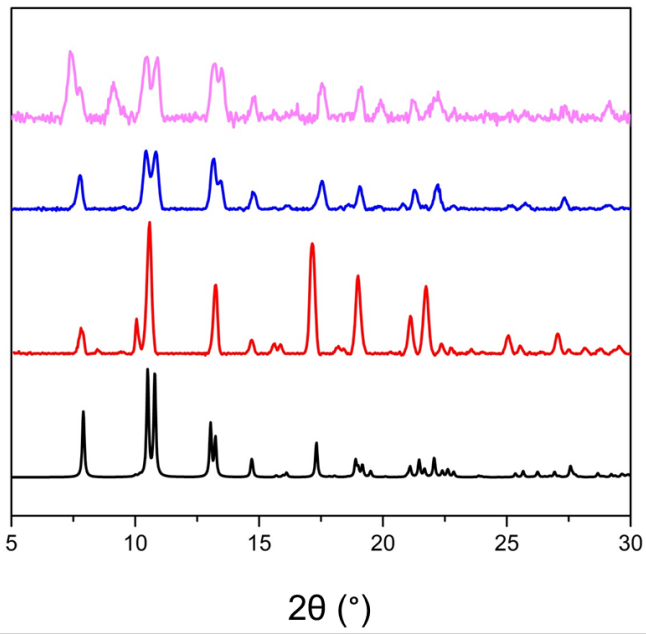

Figure S17. XRPD patterns of simulated (black) and as-synthesized (red) **1** compared to the ones obtained after heating **1** at 85 ˚C (blue) and 120 ˚C (pink) under vacuum for 24 h.

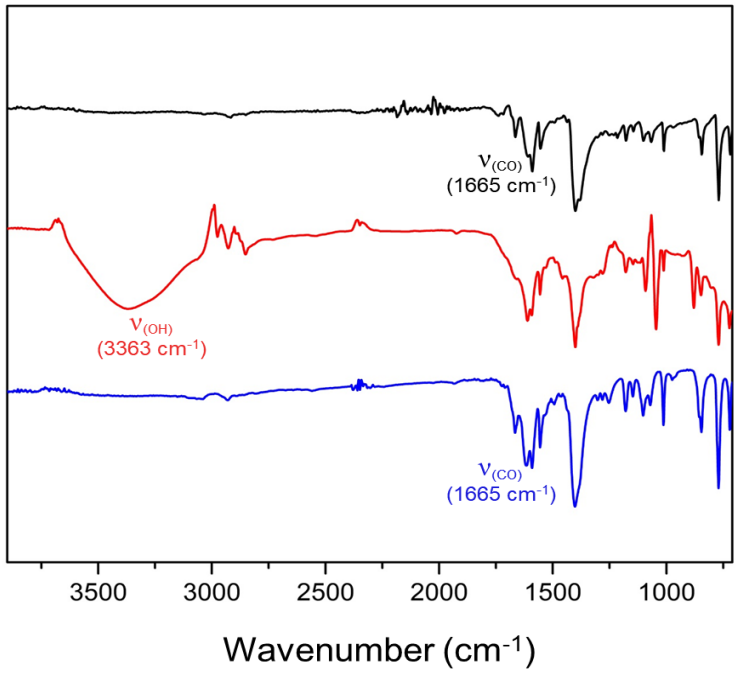

Figure S18. FT-IR spectra of **1** before (black) and after immersing in MeOH (**1´**, red) and after heating 1´ at 85 ˚C for 24 h in DMF (**1**, blue).

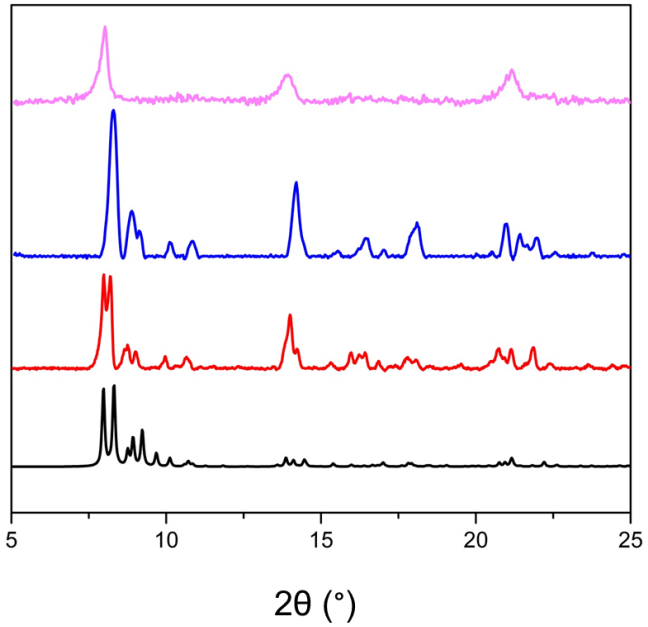

Figure S19. XRPD patterns of simulated (black) and as-synthesized (red) **2** compared to the ones obtained after heating **2** at 85 ˚C (blue) and 120 ˚C (pink) under vacuum for 24 h.

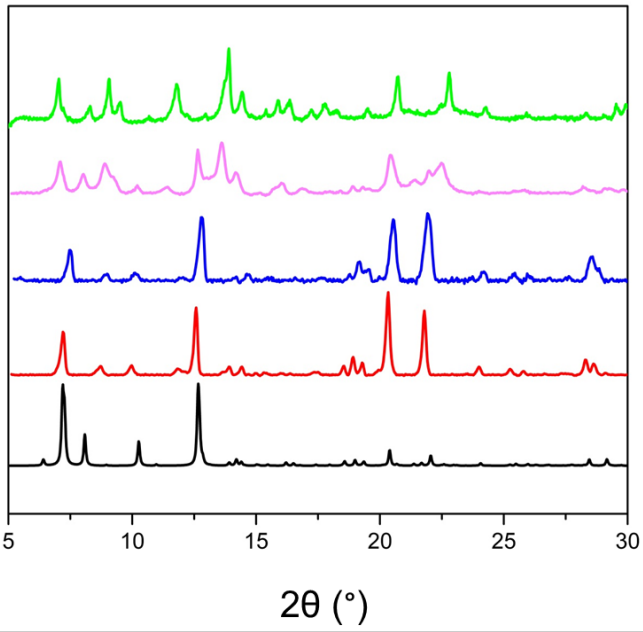

Figure S20. XRPD patterns of simulated (black) and as-synthesized (red) **3** compared to the ones obtained after heating **3** at 85 ˚C (blue) and 120 ˚C (pink) under vacuum for 24 h and as-synthesized **3´** (green).

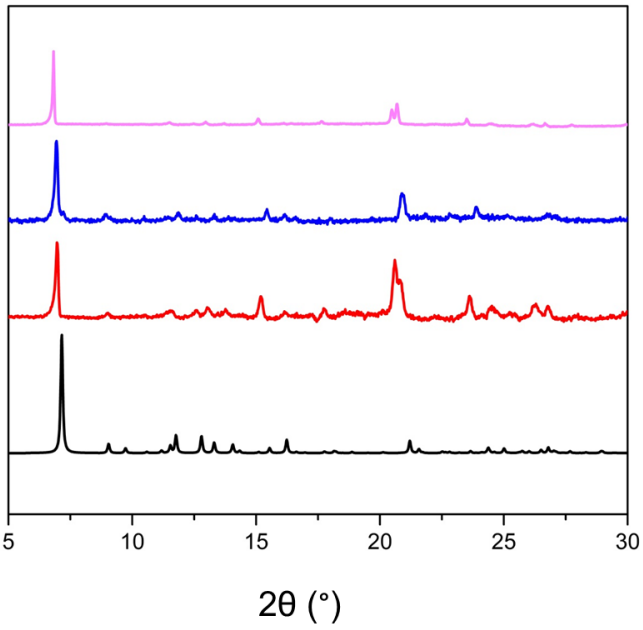

Figure S21. XRPD patterns of simulated (black) and as-synthesized (red) **4** compared to the ones obtained after heating **4** at 85 ˚C (blue) and 120 ˚C (pink) under vacuum for 24 h.

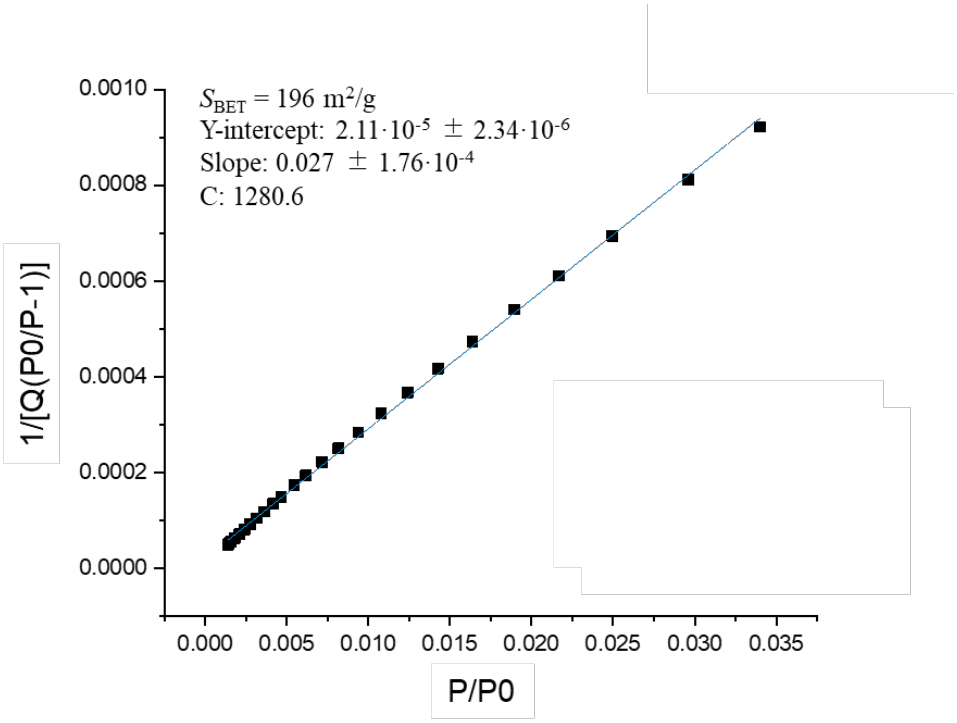

Figure S22. BET surface area plot for **1´**.

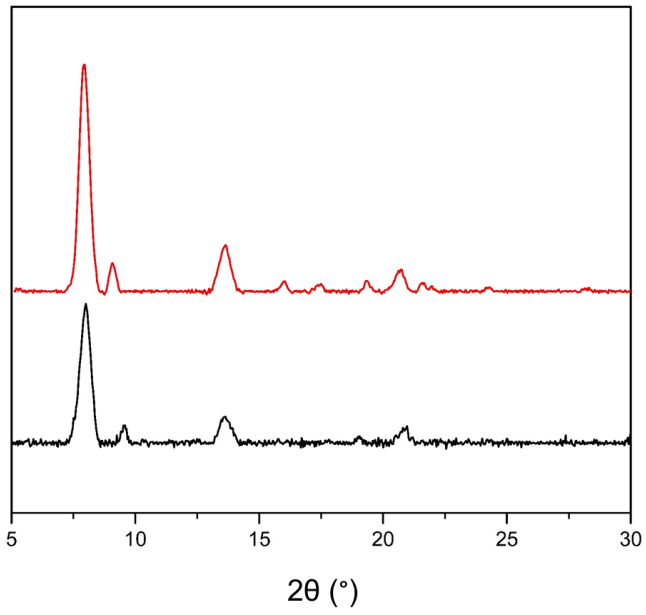

Figure S23. XRPD patterns of **1´** before (black) and after (red) adsorption. The sample was activated at 85 ˚C under vacuum for 12 h prior adsorption experiments

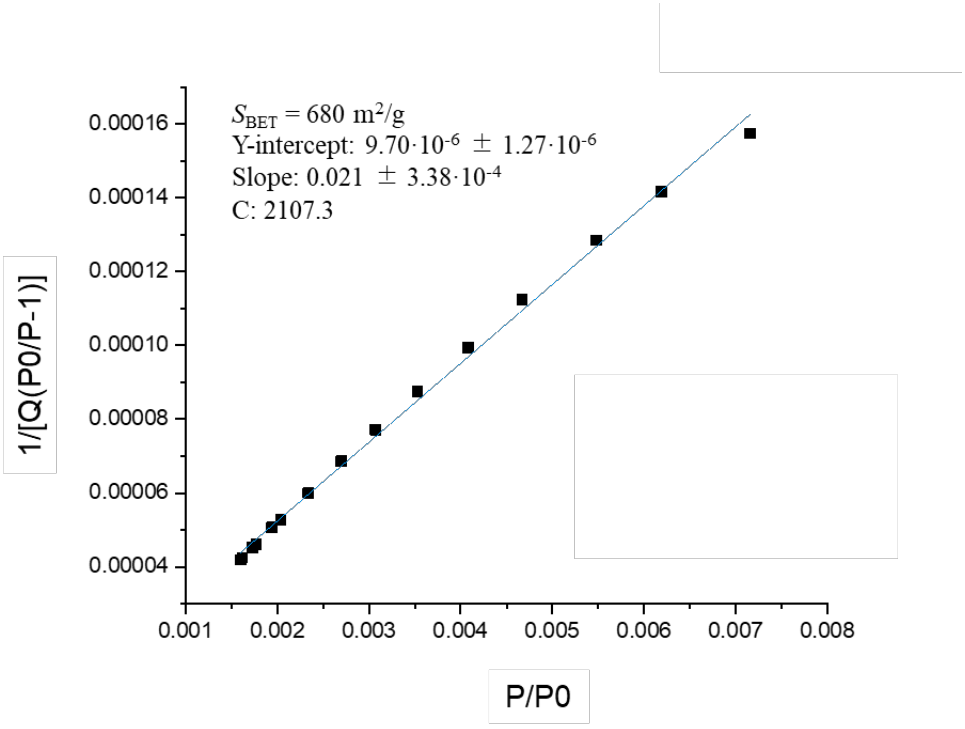

Figure S24. BET surface area plot for **3´**.

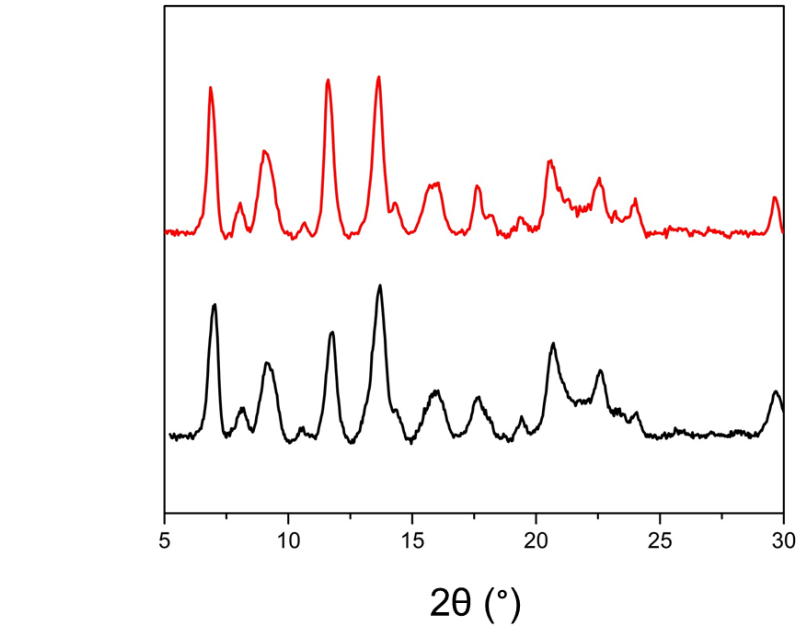

Figure S25. XRPD patterns of **3´** before (black) and after (red) adsorption. The sample was activated at 85 ˚C under vacuum for 12 h prior adsorption experiments.

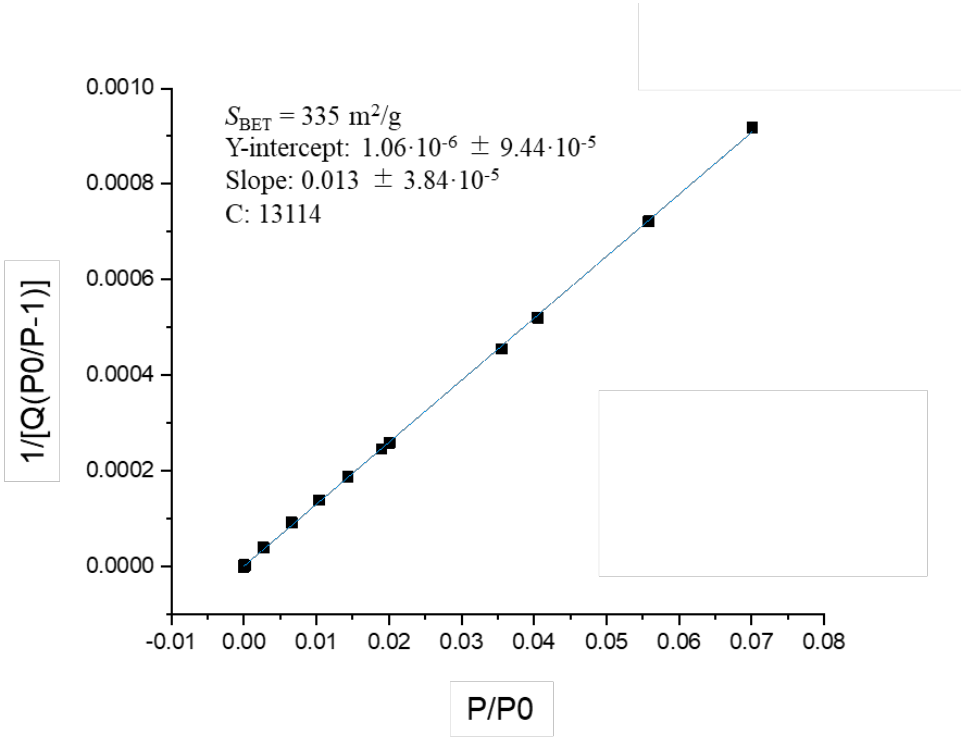

Figure S26. BET surface area plot for **4´**.

References:

(1) O.Veselska, L. Cai, D.Podbevšek, G. Ledoux, N.Guillou, G. Pilet, A. Fateeva, A. Demessence, *Inorg. Chem.,* 2018, **57**, 2736-2743.

(2) D. V.Soldatov, G. D.Enright, J. A. Ripmeester, J. Lipkowski, E. A.Ukraintseva, *J. Supramol. Chem.,* 2001, **1**, 245-251.